Journal of Applied Fluid Mechanics, Vol. 10, No. 6, pp. 1785-1798, 2017.
Available online at www.jafmonline.net, ISSN 1735-3572, EISSN 1735-3645.
DOI: 10.29252/jafm.73.245.27908

Peristaltic Pumping of a Generalized Newtonian Fluid in an Elastic Tube

A. N. S. Srinivas[1†], C. K. Selvi[1] and S. Sreenadh[2]

[1]*Department of Mathematics, School of Advanced Sciences, VIT University, Vellore, 632014, Tamilnadu, India*
[2]*Department of Mathematics, Sri Venkateswara University, Tirupati, 517502, A.P., India*

†*Corresponding Author Email: anssrinivas@vit.ac.in*

(Received April 24, 2017; accepted August 9, 2017)

ABSTRACT

The paper investigates the peristaltic pumping of an incompressible non-Newtonian fluid in an elastic tube with long wavelengths and low Reynolds number approximations. Carreau fluid model is considered for present study to describe the peristaltic flow characteristics of non- Newtonian fluid in an elastic tube. Carreau fluid is a generalized Newtonian fluid which exhibits Newtonian behaviour for $n=1$ and it resembles as a power-law model at higher shear rates. For $n<1$ it exhibits shear-thinning property, i.e., the apparent viscosity reduces with increasing shear rate. The equations governing the fluid flow are solved with usual perturbation expansion by taking Weissenberg number W_i as a perturbation parameter. The expressions for axial velocity, stream function and volume flow rate as function of pressure difference are derived. The effects of various pertinent parameters on variation of flux for a Carreau fluid flow through an elastic tube along with peristalsis are calculated and interpreted through graphs. The pressure rise per wavelength and shear stress distribution for different values of physical parameters are calculated and presented. Trapping phenomenon is presented graphically to understand the physical behaviour of various parameters. The difference in flux variation is examined by two different models of Rubinow and Keller (1972) and Mazumdar (1992). It is observed that in elastic tubes, the flux of Carreau fluid with peristalsis is more when the tension relation is a fifth degree polynomial as compared to exponential curve. When the power-law index $n=1$ or Weissenberg number $W_i=0$ and without peristalsis, the present results are similar to the observations of Rubinow and Keller (1972). Further, the relation between the function $g(a)$ and radius of the elastic tube for both Newtonian, non-Newtonian cases are discussed graphically and these findings are identical with the investigations of Mazumdar (1992). The results observed for the present flow characteristics reports several interesting behaviours that warrant further study of physiological fluids in elastic tubes with peristalsis.

Keywords: Peristaltic flow; Elastic tube; Non-newtonian fluid; Weissenberg number; Power-law index.

NOMENCLATURE

a_0	radius of the tube without elasticity	$p(z)$	pressure of the fluid
a''	change in the tube radius due to elasticity nature	$\bar{q}$	dimensional flux in fixed frame
		$(\bar{r},\bar{z})$	moving coordinates
a'	change in the tube radius due to peristaltic nature	$(\bar{R},\bar{Z})$	stationary coordinates
		t	time
b	amplitude of the wave	t_1,t_2,k,A	elastic parameters
c	wave speed	T	tension of the tube wall
F	dimensionless flux in moving frame	W_i	weissenberg number
L	length of the tube	$(\bar{w},\bar{u})$	velocity components in moving frame
n	power-law Index	$(\bar{W},\bar{U})$	velocity components in stationary frame
P	pressure gradient		
p_0	external pressure		
p_1	inlet pressure	$\bar{\dot{\gamma}}_{ij}$	strain rate tensor
p_2	outlet pressure		

ψ	stream function
Γ	time constant
λ	wave length of the peristaltic wave
δ	wave number
ϕ	amplitude ratio
θ	azimuthal angle
$\bar{\tau}_{ij}$	components of extra stress tensor in stationary frame
σ	conductivity
ρ	density
η_∞	infinite-shear-rate viscosity
η_0	zero-shear-rate viscosity

1. INTRODUCTION

Most of the earlier research works were concentrated on peristaltic pumping of non-Newtonian fluids through channels/tubes to understand the flow behaviour of physiological fluids. The present study is modelled by considering the flow through an elastic tube to describe the rheological characteristics of blood flow in a small blood vessel due to their elastic nature which has many practical biomedical applications.

In physiological peristalsis, the fluids of practical interest are Newtonian and non-Newtonian fluids, depending on the various conditions. The analysis of peristaltic pumping of non- Newtonian fluids in different type of geometries has drawn more attention among researchers due to a variety of potential applications in biomedical and industrial fields. The vasomotion of small blood vessels for example, the peristalsis nature is observed in venules, arterioles and the motion in the lymphatic vessels. In view of such significant physiological and engineering applications, a numerous theoretical and experimental investigations were attempted to understand peristalsis mechanism by various researchers for different fluids under different conditions. After the first experimental investigation of Latham (1966) on peristaltic pumping, Shapiro *et al*. (1969) presented a detailed analysis of peristaltic flow of Newtonian fluid along with experimental results.

The perturbation solution in powers of amplitude ratio was applied by Burns and Parkes (1967) in two different cases, one is the peristaltic motion without pressure gradient and another one is flow under prescribed pressure with sinusoidally varying cross section in a fixed channel walls. The periodical change in the diameter of vasomotion of blood vessels involving peristalsis was considered by Fung and Yih (1968).The shear- thinning and shear–thickening fluid effects on peristaltic pump by lubrication analysis are investigated by Rao and Mishra (2004).The theoretical analysis of MHD peristaltic transport of Jeffrey fluid along with endoscope and magnetic effects was presented by Hayat *et al*. (2008).Some investigations on peristaltic flow of different physiological fluids are reported in earlier studies. (See Radhakrishnamacharya 1982, 2007, Vajravelu et. al. 2005a, 2005b, Srinivas *et al.* 2009, 2011, Hayat *et al*. 2010, Nadeem and Akbar 2009) Poiseuille-law is considered in the study of Newtonian fluids since it explains the flux and pressure difference relationship. This relation is a linear in the case of incompressible viscous fluid flow through a tube of constant cross section. But in the most of the vascular systems, the pressure flow relation is always nonlinear due to elastic nature of blood vessel. Since most of the physiological systems are elastic in nature and non-Newtonian fluid flow through such complex geometries has drawn some important applications like blood flow in a small blood vessel, lymphatic vessel etc. A number of different methods are employed to study flow through the tubes having elastic nature under different conditions. Roach and Burton (1957) conducted an experiment on human external iliac artery to study the static pressure-volume relation as tension versus length curve and explained the reasons for distensibility of shape of arteries. Whirlow and Rouleau (1965) considered that tube as a thick-walled cylinder of visco-elastic material. Rubinow and Keller (1972) given the detailed analysis of blood flow applications by considering viscous fluid flow through elastic tube. Further, an equilibrium condition to determine tension as a function of tube radius was presented. Pandey and Chaube (2010) considered the flexible tube of changing cross section to study the Maxwell fluid flow characteristics with peristalsis. Takaghi and Balmforth (2011) applied lubrication analysis to model the deformation of the tube wall and they determined the pumping efficiency. Ali *et al*. (2016) examined the peristaltic flow characteristics of bio rheological fluids using numerical simulations.

Most of the earlier investigations were made by considering blood as Newtonian fluid that is valid for fluids with shear rate more than 100 S^{-1} which occurs in the case of large arteries. The study of variations in flow characteristics is of considerable research interest due to the non-Newtonian nature of blood flow through small arteries. The non-Newtonian behaviour of blood at lower shear rates was analysed by Pedley (1980).The experimental attempt was made by Johnson *et al*. (2004) that the Carreau fluid is appropriate model to understand the nature of blood flows in arteries. Modelling the blood flows through elastic arteries was presented by (Wang *et al.* 1992, Sharma *et al*. 2004). Akbar and Nadeem (2014) considered Carreau fluid model to analyze the blood flow through a tapered artery with a stenosis. The flow characteristics of Carreau fluid in different geometries and elasticity effects of tubes under different conditions have been studied. (See Misery *et al*. 1996, Hakeem *et al*. 2002, Mishra and Ghosh 2003, Hakeem *et al*. 2006, Sankara and Jayaraman 2001) Vajravelu *et al*. (2011) considered the case of inserting a catheter in to an elastic tube to observe the variations in blood flow pattern by taking Herschel – Bulkley fluid. Nahar *et al.* (2013) presented

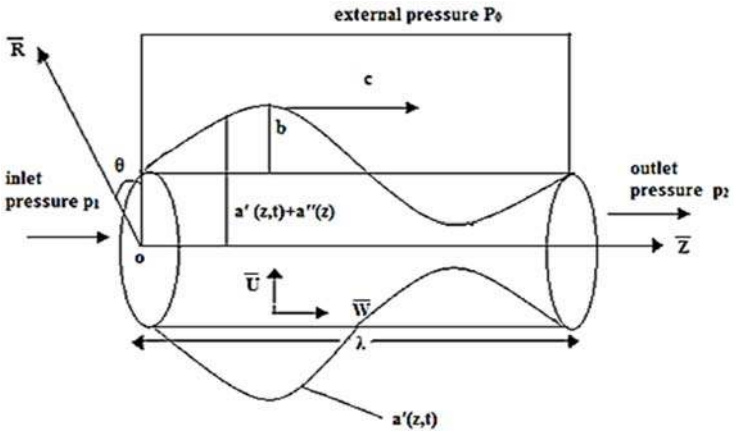

Fig. 1. Physical Model.

experimental results on non – Newtonian flow characteristics in collapsible elastic tubes. Sochi (2014) used lubrication approximation to understand the flow behaviour of Newtonian fluid and power-law fluid in elastic tubes by considering the pressure-area constitutive relation. The effect of peristalsis on Herschel –Bulkley fluid flow in an elastic tube was discussed by Vajravelu *et al.* (2014). Sochi (2015) derived analytical expressions for the Newtonian flow characteristics by considering cylindrically shaped elastic tubes. Shen *et al.* (2016) presented an elastic tube model to study the pulsatile flow characteristics of blood by taking arterial wall motion in to consideration. Further Vajravelu *et al.* (2016) investigated the Casson fluid flow through an elastic tube with peristalsis and they analyzed that Rubinow and Keller model is better than the Mazumdar model.

Motivated by the above studies, it is important to study the peristaltic pumping of generalized Newtonian fluid through elastic tube which has significant physiological applications like flow through elastic arteries etc. The problem is formulated under the assumptions that the wave number is very small and flow is to be of inertial free. The usual perturbation expansion is applied to solve the governing equations. The influence of different pertinent parameters on flux are evaluated numerically and analyzed through graphs. The variations of flux for different physical parameters are calculated using two models Rubinow and Keller, Mazumdar model. By using the above two models, the obtained results are compared graphically.

2. MATHEMATICAL FORMULATION

The peristaltic pumping of an incompressible steady Carreau fluid through elastic tube with radius $a(z)$ and length L is considered as shown in Fig.1. The flow is produced by an infinite sinusoidal wave train propagating with constant wave speed c along the tube walls. The instantaneous radius of the tube at any axial station z is represented as

$$\bar{R} = \bar{a}'(\bar{z},\bar{t}) = a_0 + b\sin\frac{2\pi}{\lambda}(\bar{Z} - c\bar{t}) \tag{2.1}$$

where a_0 is tube radius in the absence of elasticity, b is amplitude of wave, $\bar{t}$ is the time. Here the cylindrical coordinate system $(\bar{R},\theta,\bar{Z})$ is chosen where $\bar{Z}$ – axis is taken along the centre line of the tube, $\bar{R}$ is the radius of the tube and θ is azimuthal angle. By considering the approximations that the length of the tube is an integral multiple of wavelength λ, the flow is unsteady in the stationary frame and it is assumed to be steady in the moving frame of reference. The transformation between stationary coordinates $(\bar{R},\bar{Z})$ and moving coordinates $(\bar{r},\bar{z})$ is given by

$$\bar{w} = \bar{W} - c;\ \ \bar{u} = \bar{U};\ \ \bar{z} = \bar{Z} - c\bar{t};\ \ \bar{r} = \bar{R}; \tag{2.2}$$

Here $\bar{U},\bar{W}$ are the radial and axial velocity components in fixed coordinates. $\bar{u},\bar{w}$ are the radial and axial velocity components in moving coordinates.

The continuity equation and equations of motion in moving frame are given by

$$\frac{1}{\bar{r}}\frac{\partial(\bar{r}\bar{u})}{\partial\bar{r}} + \frac{\partial\bar{w}}{\partial\bar{z}} = 0 \tag{2.3}$$

$$\frac{\partial\bar{p}}{\partial\bar{r}} = -\left[\frac{1}{\bar{r}}\frac{\partial(\bar{r}\bar{\tau}_{11})}{\partial\bar{r}} + \frac{\partial\bar{\tau}_{31}}{\partial\bar{z}} - \frac{\bar{\tau}_{22}}{\bar{r}}\right] \tag{2.4}$$

$$\frac{\partial\bar{p}}{\partial\bar{z}} = -\left[\frac{1}{\bar{r}}\frac{\partial(\bar{r}\bar{\tau}_{13})}{\partial\bar{r}} + \frac{\partial\bar{\tau}_{33}}{\partial\bar{z}}\right] \tag{2.5}$$

The constitutive equation for Carreau fluid is expressed as

$$\bar{\tau}_{ij} = -\left[\eta_\infty + (\eta_0 - \eta_\infty)\left((1 + (\Gamma\bar{\dot{\gamma}})^2\right)^{\frac{(n-1)}{2}}\right]\bar{\dot{\gamma}}_{ij} \tag{2.6}$$

Here $\bar{\tau}_{ij}$, $i,j = 1,2,3$ denotes extra stress tensor components and $\bar{\dot{\gamma}}$ is defined as

$$\bar{\dot{\gamma}} = \sqrt{\frac{1}{2}\sum_i\sum_j \bar{\dot{\gamma}}_{ij}\bar{\dot{\gamma}}_{ij}} = \sqrt{\frac{1}{2}\Gamma_{\bar{\dot{\gamma}}_{ij}}} \tag{2.7}$$

here $\Gamma_{\bar{\dot{\gamma}}}$ is the second invariant of strain-rate tensor $\bar{\dot{\gamma}}_{ij}$.

We consider the case $\Gamma_{\bar{\dot{\gamma}}} < 1$ and $\eta_\infty = 0$ in Eq. (2.6), so the extra stress tensor component is written as

$$\bar{\tau}_{ij} = -\eta_0 \left[1 + \frac{n-1}{2} \Gamma^2 \bar{\dot{\gamma}}^2 \right] \bar{\dot{\gamma}}_{ij} \tag{2.8}$$

and the components of strain-rate tensor $\bar{\dot{\gamma}}_{ij}$ are given as

$$\bar{\dot{\gamma}}_{11} = 2\frac{\partial \bar{u}}{\partial \bar{r}},\ \bar{\dot{\gamma}}_{22} = 2\frac{\bar{u}}{\bar{r}},\ \bar{\dot{\gamma}}_{33} = 2\frac{\partial \bar{w}}{\partial \bar{z}},\ \bar{\dot{\gamma}}_{13} = \bar{\dot{\gamma}}_{31} = \frac{\partial \bar{w}}{\partial \bar{r}} + \frac{\partial \bar{u}}{\partial \bar{z}} \tag{2.9}$$

The appropriate boundary conditions are

$$\text{at } \bar{r} = 0 : \frac{\partial \bar{w}}{\partial \bar{r}} = 0 \tag{2.10a}$$

$$\text{at } \bar{r} = \bar{a}' : \bar{w} = -c \tag{2.10b}$$

The non-dimensional quantities are

$$z = \frac{\bar{z}}{\lambda},\ \mathrm{Z} = \frac{\bar{Z}}{\lambda},\ r = \frac{\bar{r}}{a_0},\ R = \frac{\bar{R}}{a_0},\ t = \frac{c\bar{t}}{\lambda},\ u = \frac{\lambda \bar{u}}{a_0 c},$$
$$U = \frac{\lambda \bar{U}}{a_0 c},\ w = \frac{\bar{w}}{c},\ W = \frac{\bar{W}}{c},\ \tau_{ij} = \frac{a_0 \bar{\tau}_{ij}}{c\eta_0},\ \dot{\gamma} = \frac{a_0 \bar{\dot{\gamma}}}{c},$$
$$\dot{\gamma}_{ij} = \frac{a_0 \bar{\dot{\gamma}}_{ij}}{c}, W_i = \frac{c\Gamma}{a_0},\ p = \frac{a_0^2 \bar{p}}{c\lambda\eta_0},\ a' = \frac{\bar{a}'}{a_0},\ a'' = \frac{\bar{a}''}{a_0},$$
$$\phi = \frac{b}{a_0}, \delta = \frac{a_0}{\lambda}, F = \frac{\bar{q}}{\pi a_0^2 c}; \tag{2.11}$$

Eqs. (2.3) - (2.5) in a non- dimensional form are

$$\frac{1}{r}\frac{\partial (ru)}{\partial r} + \frac{\partial w}{\partial z} = 0 \tag{2.12}$$

$$\frac{\partial p}{\partial r} = -\left[\delta \frac{1}{r}\frac{\partial (r\tau_{11})}{\partial r} + \delta^2 \frac{\partial \tau_{31}}{\partial z} - \delta \frac{\tau_{22}}{r} \right] \tag{2.13}$$

$$\frac{\partial p}{\partial z} = -\left[\frac{1}{r}\frac{\partial (r\tau_{13})}{\partial r} + \delta \frac{\partial \tau_{33}}{\partial z} \right] \tag{2.14}$$

The dimension less boundary conditions are

$$\text{at } r = 0 : \frac{\partial w}{\partial r} = 0 \tag{2.15a}$$

$$\text{at } r = a' : w = -1 \tag{2.15b}$$

The components of rate of strain tensor and extra stress tensor are

$$\dot{\gamma}_{11} = 2\delta \frac{\partial u}{\partial r},\ \dot{\gamma}_{22} = 2\delta \frac{u}{r},$$
$$\dot{\gamma}_{33} = 2\delta \frac{\partial w}{\partial z},\ \dot{\gamma}_{13} = \dot{\gamma}_{31} = \delta^2 \frac{\partial u}{\partial z} + \frac{\partial w}{\partial r} \tag{2.16}$$

$$\tau_{ij} = -\left[1 + \frac{n-1}{2} W_i^2 \dot{\gamma}^2 \right] \dot{\gamma}_{ij} \tag{2.17}$$

$$\dot{\gamma} = \sqrt{\frac{1}{2}\sum_i \sum_j \dot{\gamma}_{ij}\dot{\gamma}_{ij}} \tag{2.18}$$

Neglecting the wave number δ, the equations of motion and extra stress tensor becomes,

$$\frac{1}{r}\frac{\partial (ru)}{\partial r} + \frac{\partial w}{\partial z} = 0 \tag{2.19}$$

$$\frac{\partial p}{\partial r} = 0 \tag{2.20}$$

$$\frac{\partial p}{\partial z} = -\left[\frac{1}{r}\frac{\partial (r\tau_{13})}{\partial r} \right] \tag{2.21}$$

$$\tau_{13} = \tau_{31} = -\left[1 + \frac{n-1}{2} W_i^2 \left(\frac{\partial w}{\partial r} \right)^2 \right] \left(\frac{\partial w}{\partial r} \right) \tag{2.22}$$

eliminating pressure from Eqs. (2.20) and (2.21), we have

$$\frac{\partial}{\partial r}\left[\frac{1}{r}\frac{\partial (r\tau_{13})}{\partial r} \right] = 0 \tag{2.23}$$

3. SOLUTION

To obtain the perturbation solution the following quantities are expanded in powers of perturbation parameter W_i^2 as

$$u = u_0 + W_i^2 u_1 + O(W_i^4) \tag{3.1}$$

$$w = w_0 + W_i^2 w_1 + O(W_i^4) \tag{3.2}$$

$$\frac{\partial p}{\partial z} = \frac{\partial p_0}{\partial z} + W_i^2 \frac{\partial p_1}{\partial z} + O(W_i^4) \tag{3.3}$$

$$\tau_{13} = \tau_{13}^{(0)} + W_i^2 \tau_{13}^{(1)} + O(W_i^4) \tag{3.4}$$

$$F = F_0 + W_i^2 F_1 + O(W_i^4) \tag{3.5}$$

using Eqs. (3.1) - (3.4) in the Eqs. (2.19), (2.21), (2.22) and (2.23) results two systems of different order.

Zero Order System (Newtonian System)

$$\frac{1}{r}\frac{\partial (ru_0)}{\partial r} + \frac{\partial w_0}{\partial z} = 0 \tag{3.6}$$

$$\frac{\partial p_0}{\partial z} = -\left[\frac{1}{r}\frac{\partial (r\tau_{13}^{(0)})}{\partial r} \right] \tag{3.7}$$

$$\tau_{13}^{(0)} = -\left(\frac{\partial w_0}{\partial r} \right) \tag{3.8}$$

$$\frac{\partial}{\partial r}\left[\frac{1}{r}\frac{\partial (r\tau_{13}^{(0)})}{\partial r} \right] = 0 \tag{3.9}$$

with dimensionless boundary conditions

$$\text{at} \quad r=0: \frac{\partial w_0}{\partial r}=0 \tag{3.10a}$$

$$\text{at} \quad r=a': w_0=-1 \tag{3.10b}$$

First Order System (Non- Newtonian System)

$$\frac{1}{r}\frac{\partial (ru_1)}{\partial r}+\frac{\partial w_1}{\partial z}=0 \tag{3.11}$$

$$\frac{\partial p_1}{\partial z}=-\left[\frac{1}{r}\frac{\partial (r\tau_{13}^{(1)})}{\partial r}\right] \tag{3.12}$$

$$\tau_{13}^{(1)}=-\left(\frac{\partial w_1}{\partial r}+\frac{n-1}{2}\left(\frac{\partial w_0}{\partial r}\right)^3\right) \tag{3.13}$$

$$\frac{\partial}{\partial r}\left[\frac{1}{r}\frac{\partial (r\tau_{13}^{(1)})}{\partial r}\right]=0 \tag{3.14}$$

with dimensionless boundary conditions

$$\text{at} \quad r=0: \frac{\partial w_1}{\partial r}=0 \tag{3.15a}$$

$$\text{at} \quad r=a': w_1=0 \tag{3.15b}$$

solving the Eqs. (3.6) - (3.9) and Eqs. (3.11) - (3.14) using the dimensionless boundary conditions Eq. (3.10) and Eq. (3.15) results

$$w_0=\frac{1}{4}\left(\frac{dp_0}{dz}\right)\left(r^2-a'^2\right)-1 \tag{3.16}$$

$$w_1=\frac{1}{4}\left(\frac{dp_1}{dz}\right)\left(r^2-a'^2\right)-\frac{n-1}{2}\left(\frac{dp_0}{dz}\right)^3\left(\frac{r^4-a'^4}{32}\right) \tag{3.17}$$

using Eq. (3.2) the axial velocity w is given as

$$w=-1+\left(\frac{-8F}{a'^4}-\frac{8}{a'^2}\right)\left(\frac{r^2-a'^2}{4}\right)+\frac{(n-1)W_i^2}{4}\left(\frac{-8F}{a'^4}-\frac{8}{a'^2}\right)^3\left(\frac{a'^2(r^2-a'^2)}{12}-\frac{(r^4-a'^4)}{16}\right) \tag{3.18}$$

From Eq. (3.18), the expression for stream function is obtained by using $\left(w=\frac{1}{r}\left(\frac{\partial \psi}{\partial r}\right), u=-\frac{1}{r}\left(\frac{\partial \psi}{\partial z}\right)\right)$ and $\psi=0$ at $r=0$

$$\psi=-\frac{r^2}{2}+\left(-\frac{8F}{a'^4}-\frac{2}{a'}\right)\left(\frac{r^4}{4}-\frac{a'^2r^2}{2}\right)+\frac{(n-1)W_i^2a'^2}{48}\left(-\frac{8F}{a'^4}-\frac{8}{a'^2}\right)^3\left(\frac{r^4}{4}-\frac{a'^2r^2}{2}\right)-\frac{(n-1)W_i^2}{64}\left(-\frac{8F}{a'^4}-\frac{8}{a'^2}\right)^3\left(\frac{r^6}{6}-\frac{a'^5r^2}{2}\right) \tag{3.19}$$

The instantaneous volume flow rates for zeroth and first order F_0 and F_1 through any cross section are

$$F_0=2\int_0^{a'} rw_0\, dr \tag{3.20}$$

$$F_1=2\int_0^{a'} rw_1\, dr \tag{3.21}$$

substituting Eqs. (3.16) and (3.17) in Eqs. (3.20) and (3.21), we get

$$F_0=-\frac{a'^4}{8}\left(\frac{dp_0}{dz}\right)-a'^2 \tag{3.22}$$

$$F_1=-\frac{a'^4}{8}\left(\frac{dp_1}{dz}\right)+\frac{n-1}{96}\left(\frac{dp_0}{dz}\right)^3a'^6 \tag{3.23}$$

solving Eq. (3.22) and Eq. (3.23) for $\frac{dp_0}{dz}$ and $\frac{dp_1}{dz}$ respectively gives,

$$\frac{dp_0}{dz}=-\frac{8F_0}{a'^4}-\frac{8}{a'^2} \tag{3.24}$$

$$\frac{dp_1}{dz}=-\frac{8F_1}{a'^4}+\frac{n-1}{12}\left(\frac{dp_0}{dz}\right)^3a'^2 \tag{3.25}$$

using Eq. (3.3), the pressure gradient $\frac{dp}{dz}$ is expressed by

$$\frac{dp}{dz}=-\frac{8F_0}{a'^4}-\frac{8}{a'^2}-\frac{8F_1W_i^2}{a'^4}-\frac{(n-1)W_i^2}{12}\left(\frac{8F_0}{a'^4}+\frac{8}{a'^2}\right)^3a'^2 \tag{3.26}$$

replacing $F_0=F-W_i^2F_1$ in Eq. (3.26) and neglecting the terms greater than $O(W_i^2)$, we get

$$\frac{dp}{dz}=-\frac{8F}{a'^4}-\frac{8}{a'^2}-\frac{(n-1)W_i^2}{12}\left(\frac{8F}{a'^4}+\frac{8}{a'^2}\right)^3a'^2 \tag{3.27}$$

From Eq. (3.27), we determine the volume flow rate F through any cross section by considering only up to first order, which is given by

$$F=\frac{a'^6}{8a'^2+128(n-1)W_i^2}P-a'^2\left[\frac{24a'^2+128(n-1)W_i^2}{24a'^2+384(n-1)W_i^2}\right] \tag{3.28}$$

where $P=-\frac{dp}{dz}$

Equation (3.28) gives the volume flow rate for peristaltic flow of a Carreau fluid through elastic tube with radius $a'(z)$ in the absence of elasticity.

4. THEORETICAL DETERMINATION OF FLUX - APPLICATION TO BLOOD FLOW THROUGH ARTERY

In this section, the deformation of the tube wall due to elasticity is taken in to consideration along with peristalsis to determine the variation of flux. Consider the peristaltic pumping of a steady incompressible Carreau fluid through an elastic tube of length and radius $a(z)=a'+a''$ as shown in Fig.1.

Here $a(z)$ is the varying radius which consisting both peristalsis and elasticity effects. To calculate the flux of Carreau fluid through the tube having elastic nature, we use the Rubinow and Keller (1972) model. Let p_1 and p_2 represents the pressure of fluid at the entrance and exit respectively and p_0 is the external pressure. Here the inlet pressure p_1 is assumed to be greater than outlet pressure p_2. As a result of inside and outside pressure difference, the tube wall may expand or contract. Due to this elastic property of the tube wall there exist changes in the shape of cross section of tube. Hence, the conductivity σ of the tube at z depends on the pressure difference. Therefore the conductivity $\sigma = \sigma[p(z) - p_0]$ is a function of $(p(z) - p_0)$ .We assume that flux and the pressure gradient are related by the expression

$$F = \sigma(p - p_0)\left(-\frac{dp}{dz}\right) \tag{4.1}$$

from Eqs. (3.28) and (4.1) we have

$$\sigma(p - p_0) = \frac{a'^6}{8a'^2 + 128(n-1)W_i^2} \tag{4.2}$$

By taking elastic property in to consideration in addition to the peristaltic movement, the above Eq. (4.2) can be written as

$$\sigma(p - p_0) = \frac{(a' + a'')^6}{8(a' + a'')^2 + 128(n-1)W_i^2} \tag{4.3}$$

here a' and a'' denotes the tube radius with peristalsis and elasticity respectively. Since the flow is of Poiseuille type, the radius a'' is a function of $(p - p_0)$ at each cross section. The tube wall deformation due to peristaltic wave is $a'(z) = 1 + \phi \sin 2\pi z$.

Integrating Eq. (4.1) with respect to z from $z = 0$ and applying inlet condition $p(0) = p_1$, we get

$$\int\left\{F + a'^2\left(\frac{24a'^2 + 128(n-1)W_i^2}{24a'^2 + 384(n-1)W_i^2}\right)\right\}dz = \int_{p(z)-p_0}^{p_1-p_0} \sigma(p')dp' \tag{4.4}$$

here $p' = p(z) - p_0$. The above Eq. (4.4) determines $p(z)$ implicitly in terms of F and z . In Eq. (4.4), we take $z = 1$ and $P(1) = p_2$ to find the flux F as

$$F + 1 + \frac{\phi^2}{2} - \frac{\phi}{\pi} - \frac{32W_i^2(n-1)}{3} = \int_{p(1)-p_0}^{p_1-p_0} \sigma(p')dp' \tag{4.5}$$

substituting Eq. (4.3) in Eq. (4.5)

$$F + 1 + \frac{\phi^2}{2} - \frac{\phi}{\pi} - \frac{32W_i^2(n-1)}{3} = \int_{p_2-p_0}^{p_1-p_0} \frac{(a' + a'')^6}{8(a' + a'')^2 + 128(n-1)W_i^2}dp' \tag{4.6}$$

We can evaluate the Eq. (4.6), if the function of the form $a''(p - p_0)$ is known.

If the tension in the tube wall $T(a'')$ is a known function of a'' then $a''(p')$ can be obtained from the equilibrium condition using Rubinow and Keller (1972) model.

$$T(a'')/a'' = p - p_0 \tag{4.7}$$

4.1. Rubinow and Keller Model

The static pressure – volume relation is determined by Roach and Burton (1957) which is converted in to a tension versus length curve. This relation is represented by the following equation using Rubinow and Keller model (1972)

$$T(a'') = t_1(a'' - 1) + t_2(a'' - 1)^5 \tag{4.8}$$

where $t_1 = 13$ and $t_2 = 300$

Now substituting Eq. (4.7) in Eq. (4.8) we have,

$$dp' = \left[\frac{t_1}{a''^2} + t_2\left(4a''^3 - 15a''^2 + 20a'' - 10 + \frac{1}{a''^2}\right)\right]da'' \tag{4.9}$$

substituting Eq. (4.9) in Eq. (4.6), we evaluated the integral numerically from $p_2 - p_0$ to $p_1 - p_0$ using Mathematica software and neglecting the terms greater than $O(W_i^2)$.

The flux is given as,

$$F + 1 + \frac{\phi^2}{2} - \frac{\phi}{\pi} - \frac{32W_i^2(n-1)}{3} = \frac{1}{8}\left(g(a_1'') - g(a_2'')\right) \tag{4.10}$$

where

$$\begin{aligned} g(a) = \Bigg\{ & -\frac{(t_1 + t_2)a'^6}{(16W_i^2(n-1) + a'^2)a''} \\ & -2\left(\begin{matrix} t_1\left(8W_i^2(n-1) - 3a'^2\right) + t_2(W_i^2(n-1)(8 - 80a'^2) \\ +a'^2(-3 + 5a'^2) \end{matrix}\right)a'' \\ & +2\left(t_1a' + t_2\left(\begin{matrix} a' - 80(W_i^2(n-1))(a'-1)a' \\ -10a'^3 + 5a'^4 \end{matrix}\right)\right)a''^2 \\ & +\frac{1}{3}\left(t_1 + t_2\left(\begin{matrix} 1 - 60a'^2 + 80a'^3 - 15a'^4 \\ +80\left(W_i^2(n-1)\right)\left(2 - 8a' + 3a'^2\right) \end{matrix}\right)\right)a''^3 \\ & +t_2\left(\begin{matrix} -8\left(W_i^2(n-1)\right)\left(10 - 15a' + 2a'^2\right) \\ +a'\left(-10 + 30a' - 15a'^2 + a'^3\right) \end{matrix}\right)a''^4 \\ & +\frac{2}{5}t_2\left(\begin{matrix} -5 + 40a' - 45a'^2 + 8a'^3 \\ -8\left(W_i^2(n-1)\right)\left(-15 + 8a'\right) \end{matrix}\right)a''^5 \\ & +\frac{2}{3}\left(t_2\left(5 - 16\left(W_i^2(n-1)\right) - 15a' + 6a'^2\right)\right) \\ & a''^6 + \frac{1}{7}\left(t_2\left(-15 + 16a'\right)\right)a''^7 + \frac{1}{2}\left(t_2\right)a''^8 \\ & +\frac{4(t_1 + t_2)a'^5\left(24\left(W_i^2(n-1)\right) + a'^2\right)\log(a'')}{\left(32a'^2\left(W_i^2(n-1)\right) + a'^4\right)}\Bigg\} \end{aligned} \tag{4.11}$$

We observe that Eq. (4.11) reduces to the corresponding results of Rubinow and Keller (1972) when $W_i = 0$ or $n = 1$ and without peristalsis.

4.2. Mazumdar model:

From Mazumdar (1992), the tension relation can be expressed as

$$T(a'') = A(e^{ka''} - e^{k}) \tag{4.12}$$

where $A = 0.007435$ and $k = 5.2625$

Substituting Eq. (4.12) in (4.7), we get

$$p' = p - p_0 = \frac{1}{a''}\left[A\left(e^{ka''} - e^{k}\right)\right] \tag{4.13}$$

$$dp' = A\left(e^{ka''}\left(\frac{k}{a''} - \frac{1}{a''^2}\right) + \frac{e^{k}}{a''^2}\right)da'' \tag{4.14}$$

From Eq. (4.6) and Eq. (4.14), we have

$$F + 1 + \frac{\phi^2}{2} - \frac{\phi}{\pi} - \frac{32W_i^2(n-1)}{3} = \int_{a_2''}^{a_1''} \frac{A(a'+a'')^6}{8(a'+a'')^2 + 128(n-1)W_i^2}\left(e^{ka''}\left(\frac{k}{a''} - \frac{1}{a''^2}\right) + \frac{e^{k}}{a''^2}\right)da'' \tag{4.15}$$

The above Eq. (4.15) evaluated numerically to obtain the flux for Carreau fluid in elastic tube.

5. PUMPING CHARACTERISTICS

The pressure rise per wavelength for Carreau fluid flow through elastic tube with peristalsis is calculated using the Eqs. (4.1) and (4.3) which is given by

$$\Delta p = \int_0^1 \frac{dp}{dz}dz = \frac{-F\left[8(a'+a'')^2 + 128(n-1)W_i^2\right]}{\left(a'+a''\right)^6} \tag{5.1}$$

The non dimensional shear stress at the tube wall $r = a'$ is calculated using the Eqs. (2.22) and (3.18) which is given by

$$\tau_{ij} = -\left(\frac{-8F}{\left(a'+a''\right)^4} - \frac{8}{\left(a'+a''\right)^2}\right)\left(\frac{a'+a''}{2}\right) - \frac{(n-1)W_i^2(a'+a'')^3}{24}\left(\frac{-8F}{\left(a'+a''\right)^4} - \frac{8}{\left(a'+a''\right)^2}\right)^3 \tag{5.2}$$

6. RESULTS AND DISCUSSION

In the present analysis, the non-Newtonian Carreau fluid flow in an elastic tube in the presence of peristalsis is investigated. The effects of various pertinent parameters like fluid behaviour index n, amplitude ratio ϕ, Weissenberg number W_i, inlet elastic radius a_1'', and outlet elastic radius a_2'' on volume flow rate F are discussed graphically. For numerical computation, the choice of parameters for Carreau fluid is considered from Bird *et al.* (1977) and Tanner (1985).The volume flow rate of a non-Newtonian Carreau fluid flow through an elastic tube in the presence of both Peristalsis and elasticity nature is calculated from Eq. (4.10) using numerical computation. Figs. 2 – 6 describe the variation of flux along with z – axis by using the model of Rubinow and Keller (1972). It is noticed from Fig. 2 that, the flux enhances as the amplitude ratio ϕ increases. The variation of flux with z – axis for various values of Weissenberg number is illustrated in Fig. 3. It is clear that the volume flow rate in elastic tube for Carreau fluid is more as compared to Newtonian fluid $(W_i = 0)$. The variation of flux along the z – axis for various values of fluid behaviour index n is illustrated in Fig.4.

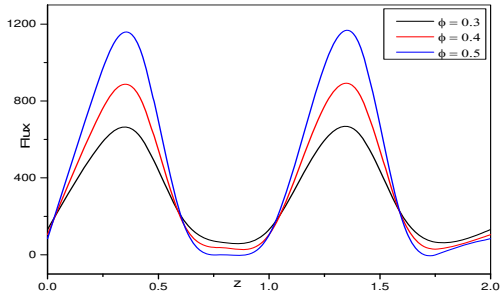

Fig.2. Flux variation F vs. z for different values of amplitude ratio ϕ with $n = 0.398$, $W_i = 0.03$, $t_1 = 13$, $t_2 = 300$, $a_1'' = 0.2$, $a_2'' = 0.3$ (by Rubinow and Keller model).

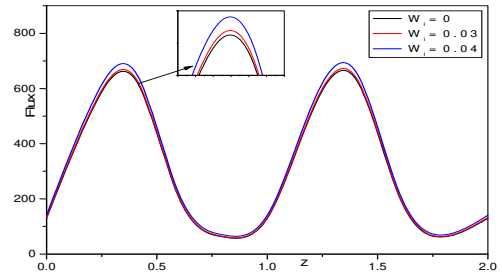

Fig. 3. Flux variation F vs. z for different values of Weissenberg number W_i with $n = 0.398$, $\phi = 0.4$, $t_1 = 13$, $t_2 = 300$, $a_1'' = 0.2$, $a_2'' = 0.3$ (by Rubinow and Keller model).

It is noticed that the there is a small variation at the maximum value of flux in an elastic tube due to non-Newtonian behaviour of Carreau fluid. That is flux is more for Carreau fluid as compared to Newtonian case $(n = 1)$. The effects of inlet and outlet elastic radius a_1'' and a_2'' on volume flow rate are presented in Figs. 5 and 6 respectively. It is noticed from Fig. 5 that, with a given fixed value for outlet elastic radius, the flux of Carreau fluid in an elastic tube decreases with increasing values of inlet elastic radius of the

tube. The opposite behaviour is observed in the case of increasing outlet elastic radius for fixed given inlet elastic radius which is shown in Fig. 6. That is increasing outlet radius increases the flux of Carreau fluid flow in an elastic tube.

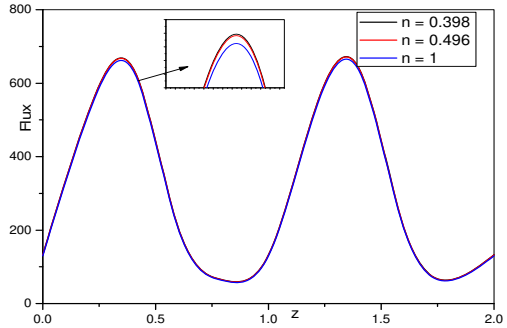

Fig. 4. Flux variation F vs. z for different values of power-law index n with $\phi = 0.4, W_i = 0.03, t_1 = 13, t_2 = 300, a_1'' = 0.2, a_2'' = 0.3$ (by Rubinow and Keller Model).

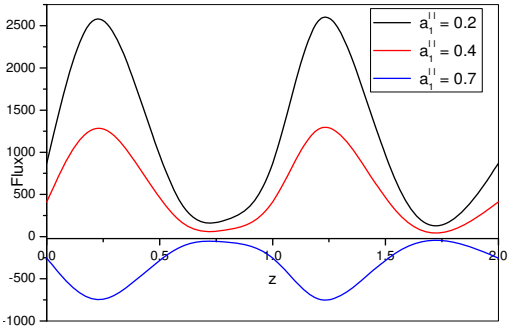

Fig. 5. Flux variation F vs. z for different values of inlet elastic radius a_1'' with $n=0.398, \phi=0.4, t_1=13, t_2 = 300, W_i = 0.03, a_2'' = 0.3$ (Rubinow and Keller model).

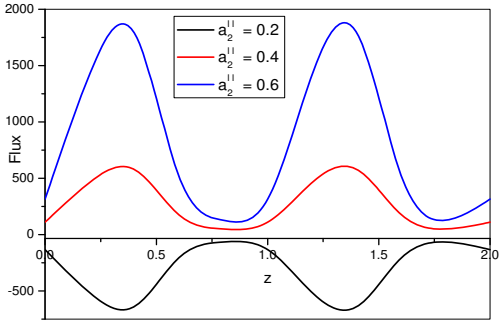

Fig. 6. Flux variation F vs. z for different values of outlet elastic radius a_2'' with $\phi=0.4, W_i = 0.03, t_1 = 13, t_2 = 300, a_1'' = 0.2, n = 0.398$ (by Rubinow and Keller model).

The variation of flux along the $z-$axis is calculated numerically using the method of Mazumdar for different pertinent parameters which are graphically described in Figs. 7-11. It is clear that the flux enhances in the case of Rubinow and Keller model (1972) when compared to the Mazumdar model (1992). That is the enhancement of flux is observed when the tension relation is a fifth degree polynomial rather than that of an exponential curve.

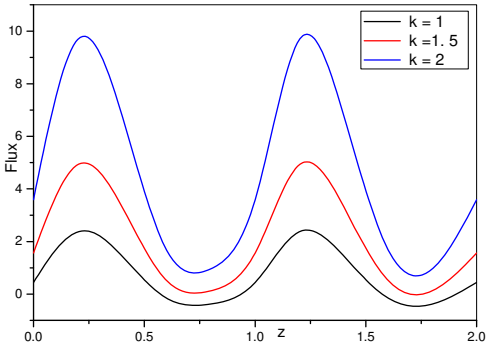

Fig. 7. Flux variation F vs. z for different values elastic parameter k with $n=0.398, \phi=0.4, A=0.007435, W_i = 0.03, a_1'' = 0.2, a_2'' = 0.3$ (by Mazumdar model).

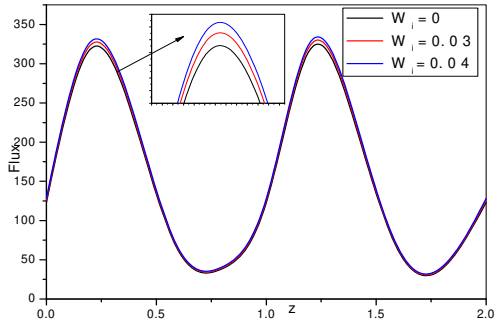

Fig. 8. Flux variation F vs. z for different values Weissenberg number W_i with $\phi = 0.4, A = 0.007435, a_1'' = 0.2, a_2'' = 0.3, n = 0.398, k = 5.2625$ (by Mazumdar model).

The Eq. (4.11) corresponds to the relationship between the function $g(a)$ and non-dimensional radius of the tube $a(z)$ with peristalsis and elasticity effects. Fig. 12 demonstrates the effect of fluid behaviour index n on the function $g(a)$ in the absence of peristalsis. We found that the values of the function $g(a)$ increases as power-law index n increases. In particular $g(a)$ values are higher for Newtonian fluid case $n=1$ when compared to Carreau fluid case $n = 0.398, 0.496$. Mazumdar (1992) examined the same relationship for a flow of a power-law fluid through an elastic tube. Our present results are similar to the analysis of Mazumdar (1992) in the absence of peristalsis. Further, the significant observation is that for

Newtonian fluid $n=1$ without peristalsis, present results are in good agreement with the investigations of Rubinow and Keller (1972). The variation of $g(a)$ for various values of Weissenberg number W_i in the absence of peristalsis is depicted in Fig. 13. It is noticed that the values of $g(a)$ reduces with increasing values of W_i. It is clear that the function $g(a)$ takes higher values for Newtonian fluid W_i as compared to Carreau fluid $W_i = 0.03, 0.04$.

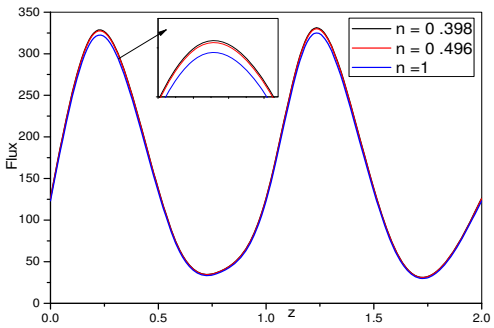

Fig. 9. Flux variation F vs. z for different values power - law index n with $k = 5.2625$, $A = 0.007435$, $\phi = 0.4$, $W_i = 0.03$, $a_1'' = 0.2$, $a_2'' = 0.3$ (by Mazumdar model).

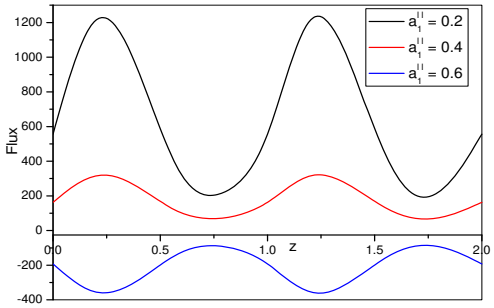

Fig. 10. Flux variation F vs. z for different values inlet elastic radius a_1'' with $\phi = 0.4$, $A = 0.007435$, $k = 5.2625$, $W_i = 0.03$, $n = 0.398$, $a_2'' = 0.3$ (by Mazumdar model).

The effect physical parameters on variation in pressure rise Δp along with flux for elastic tube are calculated using Eq. (5.1) and presented in Figs. 14-17. From Fig. 14 it is observed that for a given flux, the pressure rise per wavelength increases with increasing values of power-law index n and the maximum pressure rise is noticed for Newtonian case $(n=1)$. Also for a given pressure rise, the flux increases with increasing n. The variation in pressure rise for different values of Weissenberg number W_i is shown in Fig. 15. It is clear that for a given flux, the pressure rise decreases as W_i increases and it is maximum when $(W_i = 0)$. For a given pressure rise flux decreases as W_i increases. Fig.16. illustrates that for a given flux, the pressure rise increases as amplitude ratio ϕ increases. The variation in pressure rise for different values of elastic radius is shown in Fig.17. It is observed that for given flux, the pressure rise decreases with increasing values of elastic radius a''.

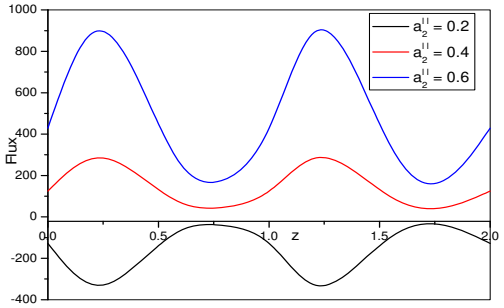

Fig. 11. Flux variation F vs. z for different values outlet elastic radius a_2'' with $k = 5.2625$, $\phi = 0.4$, $A = 0.007435$, $W_i = 0.03$, $a_1'' = 0.2$, $n = 0.398$ (by Mazumdar model).

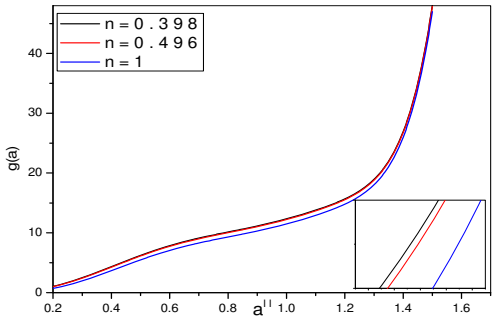

Fig. 12. The function $g(a)$ vs. a'' for different values of power – law index n with $t_1 = 13$, $t_2 = 300$, $W_i = 0.03$, $a' = 0$.

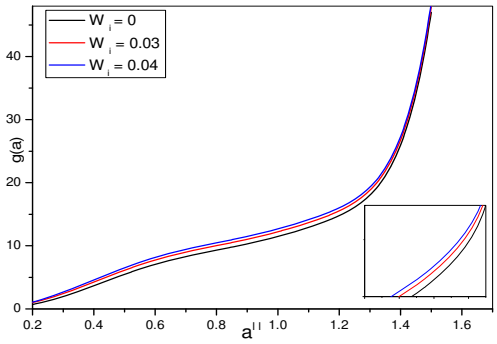

Fig. 13. The function $g(a)$ vs. a'' for different values of Weissenberg number W_i with $t_1 = 13$, $t_2 = 300$, $n = 0.398$, $a' = 0$.

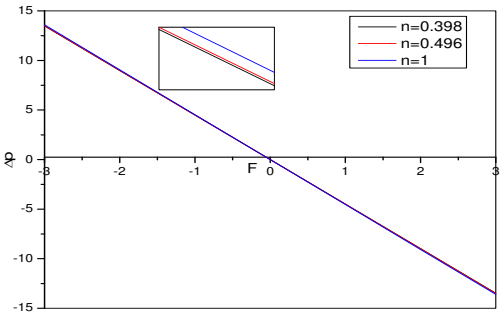

Fig. 14. The pressure rise vs. flux for different values of power-law index n with $a'' = 0.3,\ W_i = 0.03,\ \phi = 0.4$.

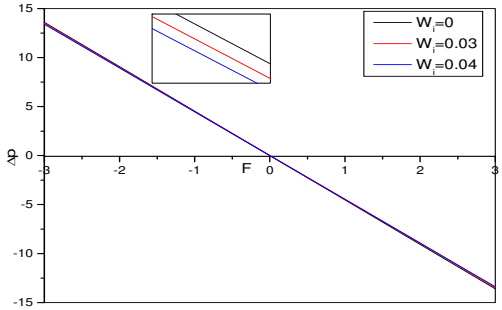

Fig. 15. The pressure rise vs. flux for different values of Weissenberg number W_i with $a'' = 0.3,\ n = 0.398,\ \phi = 0.4$.

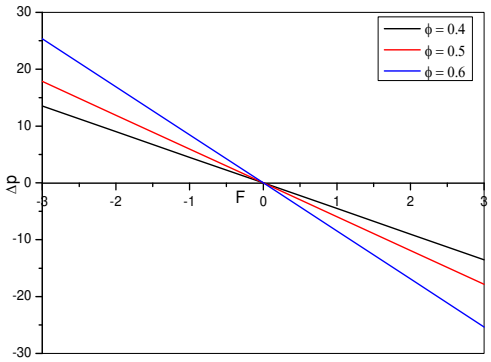

Fig. 16. The pressure rise vs. flux for different values of amplitude ratio ϕ with $a'' = 0.3,\ n = 0.398,\ W_i = 0.03$.

The shear stress distribution at the wall for different physical parameters is presented form Figs. 18-21. From Fig. 18 it is observed that shear stress increases as power-law index n increases where the opposite behaviour is observe in the case of Weissenberg number W_i . That is shear stress reduces for increasing values of W_i is shown in Fig.19. The effect of amplitude ratio ϕ on shear stress distribution is illustrated in Fig.20. It is found that shear stress increases with increasing values of ϕ .The variation in shear stress distribution for different values of elastic radius is shown in Fig. 21 and it is seen that the shear stress decreases as elastic radius parameter a'' increases.

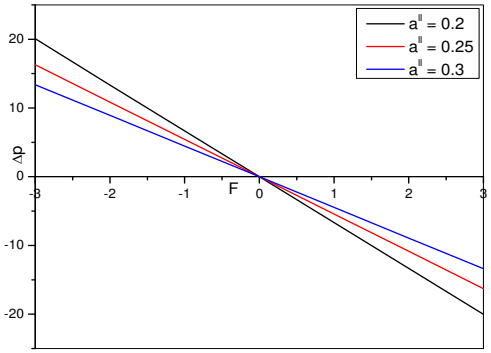

Fig. 17. The pressure rise vs. flux for different values of elastic radius a'' with $\phi = 0.4,\ n = 0.398,\ W_i = 0.03$.

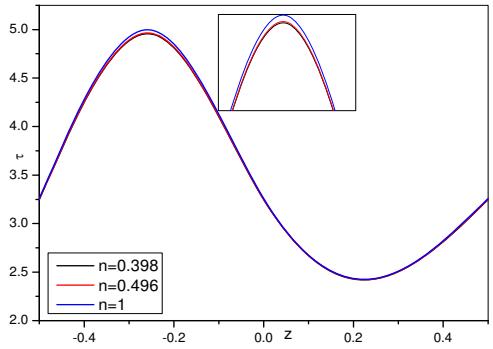

Fig. 18. The shear stress vs. z for different values of power-law index n with $\phi = 0.4,\ a'' = 0.3,\ W_i = 0.04.$

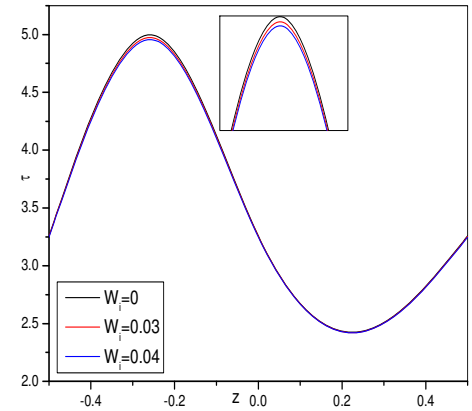

Fig. 19. The shear stress vs. z for different value of Weissenberg number W_i with $\phi = 0.4,\ a'' = 0.3,\ n = 0.398$.

Trapping is the other interesting phenomenon observed in peristalsis mechanism. The effects of different pertinent parameters on the size of trapped bolus are presented in Figs. 22-26. The variation in the size of bolus due to the Weissenberg number W_i

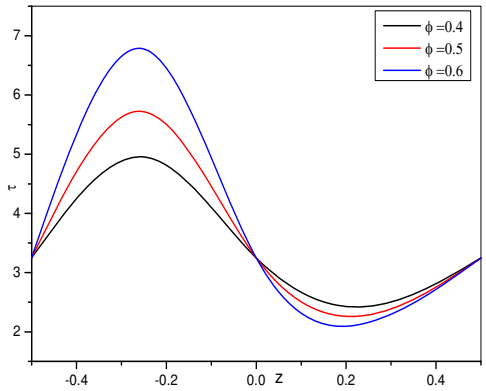

Fig. 20. The shear stress vs. z for different values of amplitude ratio ϕ with $W_i = 0.04,\ a'' = 0.3,\ n = 0.398$.

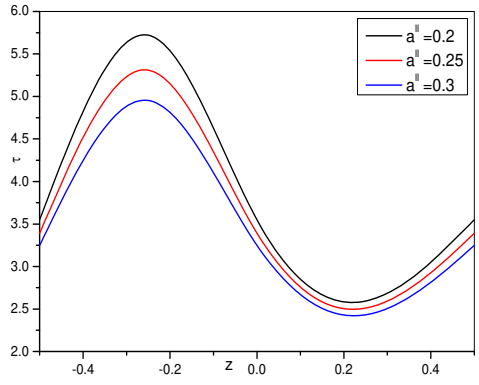

Fig. 21. The shear stress vs. z for different values of elastic radius a'' with $W_i = 0.04,\ \phi = 0.4,\ n = 0.398$.

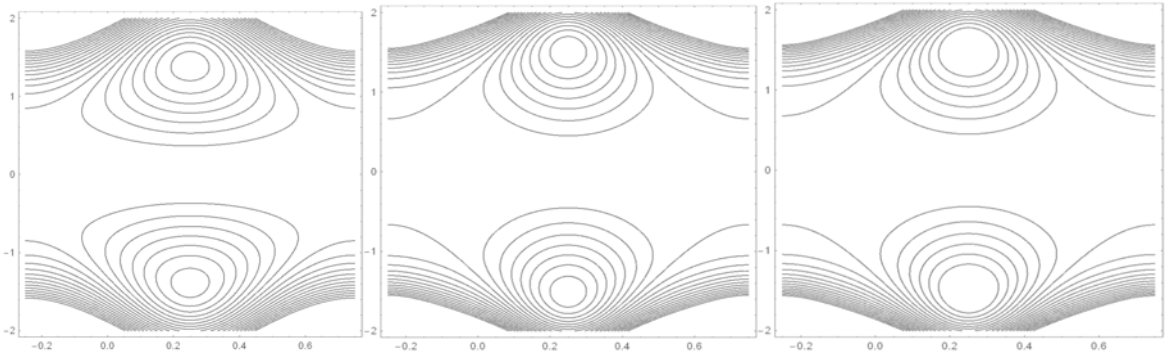

(a) (b) (c)

Fig. 22. Streamlines with $\phi = 0.4, n = 0.496, a_1'' = 0.2, a_2'' = 0.3$ and $(a)W_i = 0\ (b)W_i = 0.03\ (c)W_i = 0.04$.

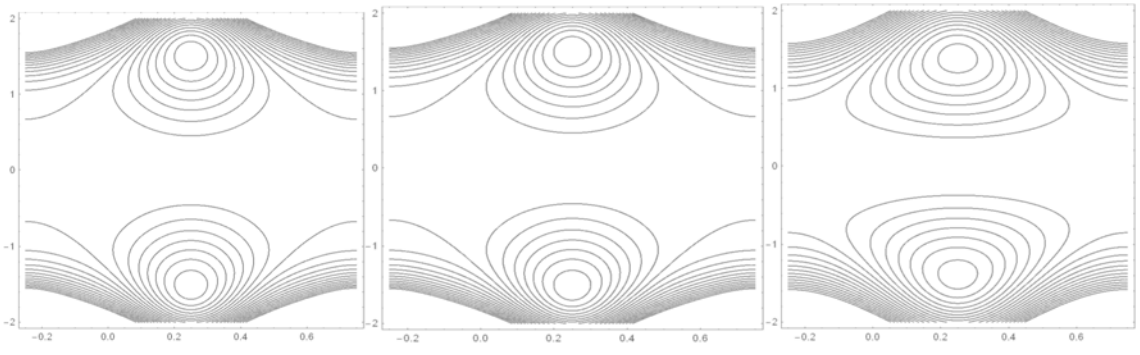

(a) (b) (c)

Fig. 23. Streamlines with $\phi = 0.4, W_i = 0.03, a_1'' = 0.2, a_2'' = 0.3$ and $(a)n = 0.398\ (b)n = 0.496\ (c)n = 1$.

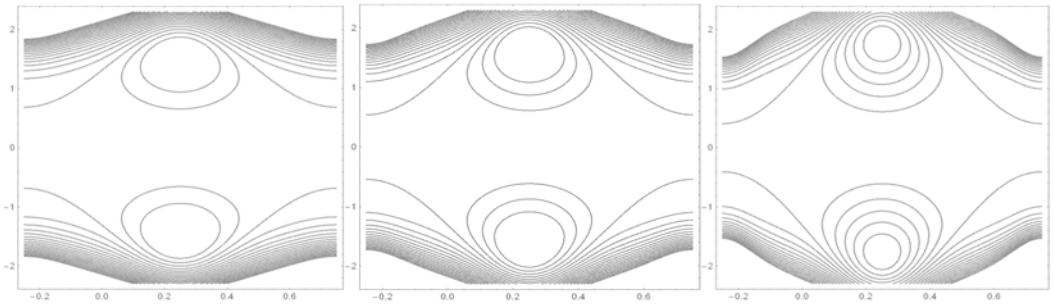

(a) (b) (c)

Fig.24. Streamlines with $n = 0.398, W_i = 0.04, a_1'' = 0.2, a_2'' = 0.3$ and $(a)\phi = 0.4$ $(b)\phi = 0.5$ $(c)\phi = 0.6$.

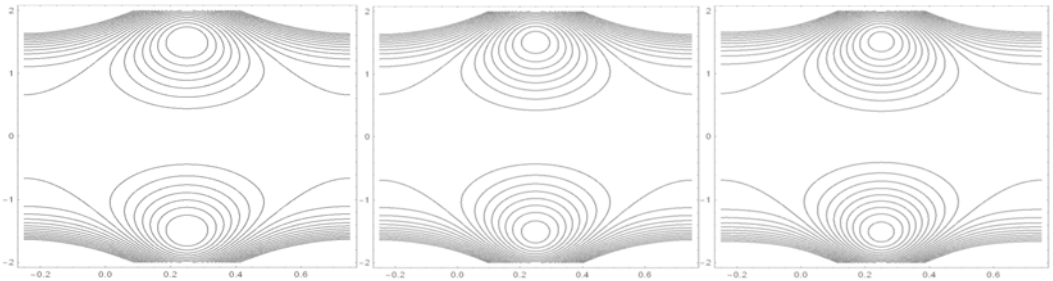

(a) (b) (c)

Fig.25. Streamlines with $n = 0.398, W_i = 0.04, \phi = 0.4, a_2'' = 0.2$ and $(a)a_1'' = 0.3$ $(b)a_1'' = 0.4$ $(c)a_1'' = 0.5$.

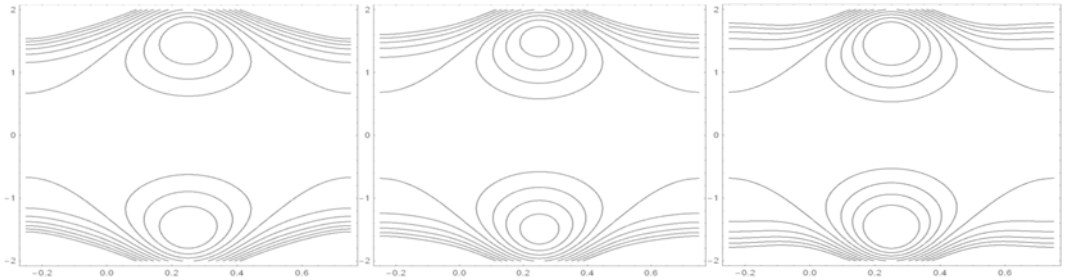

(a) (b) (c)

Fig.26. Streamlines with $n = 0.398, W_i = 0.04, \phi = 0.4, a_1'' = 0.2$ and $(a)a_2'' = 0.3$ $(b)a_2'' = 0.5$ $(c)a_2'' = 0.7$.

for fixed values of inlet and outlet elastic radius is illustrated in Fig.22.

It is clear that the bolus size reduce due to the increasing values of W_i which means that the bolus size decreases due to the non-linearity nature of Carreau fluid for $W_i = 0.03, 0.04$. The effect of power-law index n for Newtonian fluid $n = 1$ and non-Newtonian case $n = 0.398, 0.496$ are analysed from Fig. 23. It is clear that the size of the bolus is large for Newtonian fluid when compared to the non-Newtonian case through elastic tube.

Figure 24 depict the effect of amplitude ratio ϕ on size of trapped bolus for fixed given values of Weissenberg number W_i , power-law index n and elastic radius parameters a_1'' and a_2'' . The size of the bolus increases as amplitude ratio increases. The bolus size increases with increasing inlet and outlet elastic radius are presented in Figs. 25 and 26 respectively.

7. CONCLUSIONS

The present study deals with the peristaltic transport of a generalized Newtonian fluid in an elastic tube under the approximations of long wavelength and low Reynolds number. Carreau fluid model is considered as a non-Newtonian fluid due to its shear thinning behaviour. The pressure gradient, axial velocity, flow rate and shearing stress are expanded in a usual perturbation series with a Weissenberg number that contained the non-Newtonian coefficients appropriate to shear thinning. The effects of physical parameters on volume flow rate are

calculated by Rubinow and Keller model and Mazumdar model. The trapping phenomenon is explained graphically. The important observations are summarized as follows.

(i) The flux enhances with increasing values of amplitude ratio for fixed values of inlet and outlet radius parameters and flux variation is more for Carreau fluid when compared to Newtonian case.

(ii) For a given fixed value of outlet elastic radius, the flux of Carreau fluid in an elastic tube decreases with increasing values of inlet elastic radius of the tube. The opposite behaviour is observed in the case of increasing outlet elastic radius for fixed given inlet elastic radius.

(iii) The variation of flow pattern in the presence of peristalsis and elastic nature is observed by two different models namely, Rubinow and Keller model and Mazumdar model, that is the flux is much more enhanced in the Rubinow and Keller model as compared to Mazumdar model.

(iv) In the absence of peristalsis, $g(a)$ as a function of elastic tube radius takes the maximum values for Newtonian fluid $n=1$ or $W_i=0$ when compared to the Carreau fluid.

(v) For a given flux, The pressure rise increases for increasing values of power-law index and amplitude ratio where it decreases with increasing values of Weissenberg number and elastic radius.

(vi) The shear stress distribution at the wall increases with increasing values of power-law index and amplitude ratio where the opposite behaviour is noticed for increasing values of Weissenberg number and elastic radius parameter.

(vii) The bolus size is large for Newtonian fluid case as compared to Carreau fluid. The size of the tapered bolus increases with increasing values of amplitude ratio, inlet elastic radius and outlet elastic radius.

ACKNOWLEDGEMENT

The authors thank the referees for their constructive comments which lead to betterment of the article.

REFERENCES

Abd El, H. and A. E. M. El Misery (2002). Effects of an endoscope and generalized Newtonian fluid on peristaltic motion. *Appl. Math. Comp*. 128, 19-35.

Abd El, H., A. E. M. El Misery and I. E. Shamy (2006). Hydrodynamic flow of generalized Newtonian fluid through a uniform tube with peristalsis. *Appl. Math. Comp*. 173, 856-871.

Akbar, N. S. and S. Nadeem (2014). Carreau fluid model for blood flow through a tapered artery with a stenosis. *Ain Shams Engineering Journal*. 5, 1307-1316.

Ali, N., K. Javid, M. Sajid and O. Anwar Beg (2016). Numerical simulation of Peristaltic flow of a bio rheological fluid with shear - dependent viscosity in a curved channel. *Computer Methods in Biomechanics and Biomedical Engineering*. 19, 614-627.

Bird, R.B., Armstrong, R.C. and O. Hassager (1977). Dynamics of Polymeric Liquids. *, New York: John Wiley & Sons.*

Burns, J.C., and T. Parkes (1967). Peristaltic motion. *J. Fluid Mech*.29, 731-743.

Fung, Y.C. and C.S. Yih (1968). Peristaltic transport. *J. Appl. Mech*. Trans ASME. 5, 669-675.

Hayat, T. and S. Hina (2010). The influence of wall properties on the MHD Peristaltic flow of a Maxwell fluid with heat and mass transfer. *Nonlinear Anal: Real World Appl*. 11, 3155-3169.

Hayat, T., N. Ahmad and N. Ali (2008). Effects of endoscope and magnetic field on the Peristalsis involving Jeffrey fluid. *Comm. Nonlinear. Sci.Numer.Simul.*13, 1581- 1591.

Hua Shen, Yong Zhu and K. R. Qin (2016). A theoretical computerized study for the electrical conductivity of arterial pulsatile blood flow by an elastic tube model. *Medical Engineering and Physics.* 38, 1439-1448.

Johnston, B. M., P. R. Johnston, S. Corney and D. Kilpatrick (2004). Non-Newtonian blood flow in human right coronary arteries: Steady state simulations. *J. Bio Mech*. 37, 709-720.

Latham, T. W. (1966). Fluid motions in a peristaltic pump. MS thesis, Massachusetts Institute of Technology, Cambridge.

Mazumdar, N. J. (1992). Bio fluid Mechanics, *World Scientific, chapter.5*, Singapore.

Misery, A. M. E., Elsayed F. Elshehawey and A. A. Hakeem (1996). Peristaltic motion of an incompressible generalized Newtonian fluid in a planar channel. *Journal of physical Society of Japan* 65, 3524-3529.

Mishra, J. C. and S. K. Ghosh (2003). Pulsatile flow of a viscous fluid through a porous elastic vessel of variable cross-section -A mathematical model for Hemodynamic flows. *Computers and Mathematics with Applications*. 46, 947-957.

Nadeem, S. and N. S. Akbar (2009). Influence of heat transfer on a peristaltic transport of Herschel – Bulkley fluid in a non uniform inclined tube. *CNSNS*. 14, 4100-4113.

Nahar, S., S. A. K. Jeelani and E. J. Windhab (2013). Prediction of velocity profiles of shear thinning fluids flowing in elastic tubes. *Chemical Engineering Communications.* 200, 820-835.

Pandey, S. K. and M. K. Chaube (2010). Peristaltic

transport of a visco-elastic fluid in a tube of a non-uniform cross section. *Mathematical and Computer Modelling*. 52, 501-514.

Pedley, T. J. (1980). *The fluid mechanics of large blood vessels*, Cambridge University press.

Radhakrishnamacharya, G. (1982). Long wavelength approximation to peristaltic motion of a power-law fluid. *Rheologica Acta*. 21, 30-35.

Radhakrishnamacharya, G. and Ch. Srinivasulu (2007). Influence of wall properties on peristaltic transport with heat transfer. *Comptes Rendus Mecanique*. 335, 369- 373.

Rao, A. R. and M. Mishra (2004). Peristaltic transport of a power-law fluid in a porous tube. *J. Non-Newtonian Fluid Mech.* 121, 163-174.

Roach, M. R. and A. C. Burton (1957). The reason for the shape of distensibility curves of arteries, *Can. J. Biochem Physiol*. 35, 681-690.

Rubinow, S. I. and Joseph B. Keller (1972). Flow of a viscous fluid through an elastic tube with applications to blood flow. *J. theor. Biol*. 35, 299-313.

Sankar, A. and G. Jayaraman (2001). Non-linear analysis of oscillatory flow in the annulus of an elastic tube: Application to catheterized artery. *Physics of Fluids*. 13, 2901-2911.

Shapiro, A. H., M. Y. Jaffrin and S. L. Weinberg (1969). Peristaltic pumping with long wavelengths at low Reynolds number. *J. Fluid Mech.* 37, 799-825.

Sharma, G. C., M. Jain and A. Kumar (2004). Performance modelling and analysis of blood flow in elastic arteries. *Mathematical and Computer Modelling*. 39, 1491-1499.

Sochi, T. (2015). Navier - Stokes flow in cylindrical elastic tubes. *J. Appl. Fluid Mech.* 8, 181-188.

Srinivas, S. and M. Kothandapani (2009). The influence of heat and mass transfer on MHD peristaltic flow through a porous space with complaint walls. *Appl. Math. Comp.* 213, 197-208.

Srinivas, S., R. Gayathri and M. Kothandapani (2011). Mixed convective heat and mass Transfer in an asymmetric Channel with peristalsis. *Commun. Nonlinear Sci. Numer. Simul.*16, 1845-1862.

Taha, S. (2014). The flow of Newtonian and power-law fluids in elastic tubes. *Int. J. Non-linear Mechanics.* 67, 245-250.

Takagi, D. And N. J. Balmforth (2011). Peristaltic pumping of viscous fluid in an elastic tube, *J. Fluid Mech.* 672, 196-218.

Tanner, R. I. (1985). Engineering Rheology. *Oxford University press. New York*.

Vajravelu, K., S. Sreenadh and V. Ramesh Babu (2005a). Peristaltic transport of a Herschel-Bulkley fluid in an inclined tube. *Int. J. Nonlinear Mech*. 40, 83-90.

Vajravelu, K., S. Sreenadh and V. Ramesh Babu (2005b). Peristaltic pumping of Herschel-Bulkley fluid in a channel. *Appl. Math. Comp*. 169, 726-735.

Vajravelu, K., S. Sreenadh, P. Devaki and K. V. Prasad (2011). Mathematical model for a Herschel- Bulkley fluid flow in an elastic tube. *Central European Journal of Physics*.9, 1357-1365.

Vajravelu, K., S. Sreenadh, P. Devaki and K. V. Prasad (2016). Peristaltic pumping of a Casson fluid in an elastic tube. *J. Appl. Fluid Mech.* 9, 1897-1905.

Vajravelu, K., S. Sreenadh, P. Devaki and K. V. Prasad (2014). Peristaltic transport of a Herschel-Bulkley fluid in an elastic tube. *Heat Transfer-Asian Research*. 44, 585-598.

Wang, D. M. and J. M. Tarbell (1992). Non linear analysis of flow in an elastic tube (artery): Steady streaming effects. *J. Fluid Mech*. 239, 341-358.

Whirlow, D. K. and W. T. Rouleau (1965). Periodic flow of a viscous fluid in a thick-walled elastic tube. *Bulletin of Mathematical Biophysics*. 27, 355-370.